

# LOOSELY COUPLED FLUID/SOLID HEAT TRANSFER ANALYSIS USING A DYNAMIC HTC APPROACH

*R. Corral<sup>1,2</sup> - Z. Wang<sup>2</sup> - J.M. Chaquet<sup>1</sup> - G. Pastor<sup>1</sup>*

<sup>1</sup> Technology and Methods Department, Industria de TurboPropulsores S.A, Madrid, Spain 28830  
Email: roque.corral@itp.es, jose.chaquet@itp.es, guillermo.pastor@itp.es

<sup>2</sup> School of Aeronautics, UPM, Madrid, Spain, 28040  
Email: zhi.wang@upm.es

## ABSTRACT

This paper presents an improved approach of loosely coupled fluid/solid heat transfer method for the purpose of reducing computational time cost. The numerical analysis of the coupling process of an one-dimensional model, shows that the convergence behaviour is influenced by the physical Biot number and a virtual heat transfer coefficient. The novelty of the method is based on the use of dynamic evaluation of the numerical parameters of the coupling, namely the virtual heat transfer coefficient. It is shown that the computational time can be significantly reduced comparing to previous existing methods. The new approach only spends less than 2.5 times the cost of stand-alone CFD simulation of the problem to obtained a coupled fluid/solid thermal analysis.

## NOMENCLATURE

Bi	Biot number	0	initial value
<b>F</b>	the sum of the flux	i	node index
k	thermal conductivity	max	maximum
l	characteristic length	min	minimum
q	heat flux	n	number of iterations
Q	volumetric heat source	ref	reference
t	time	w	wall
T	temperature		
<b>U</b>	vector of conservative variable	<b>Abbreviation</b>	
		CFD	Computational Fluid Dynamics
<b>Greeks</b>		BEM	Boundary Element Method
$\beta$	stopping threshold	FEM	Finite Element Method
$\varepsilon$	non-dimensional convergence level	FVM	Finite Volume Method
$\eta$	convergence efficiency	hFTB	heat transfer coefficient Forward Temperature Backward
$\Omega$	domain	htc	heat transfer coefficient
<b>Scripts</b>		MAGPI	Main Annulus Gas Path Interactions
*	artificial value		

## INTRODUCTION

With rapid growth of computer power, high fidelity CFD simulations are used for helping temperature prediction in turbomachinery applications. Traditionally, the CFD analysis is uncoupled with

the metal conduction code. The CFD performs at some typical engine operating points to provide a reasonable thermal characteristics estimation at the interface wall, then this information is applied to solid thermal code for the prediction of metal temperatures and displacements. Several hypotheses are used in this process and the accuracy of this kind of methods still relies on empirical database and engineering experience. Hence, in highly complex flow cases like turbine cavity flows or internal cooling problems, those hypothesis could generate considerable errors in the temperature field estimation.

More accurate prediction can be achieved by means of coupled heat transfer method, where the solution satisfies only the temperature and heat flux continuity conditions at the fluid/solid interface. There are two main approaches of this kind. One approach is called fully coupled heat transfer method, in which the fluid equations and solid heat conduction equation are solved simultaneously in one solver. Its use in turbomachinery applications were early implemented and intensively studied by Bohn et al. (1995); Han et al. (2001); Rigby and Lepicovsky (2001). In this method, the solver realized by expanding the fluid solver function to include the solid heat conduction in solid part. In the solid region, the governing equations reduce to the heat conduction equation, by not solving mass and momentum equations, explicitly using zero velocities and using solid material specific heat coefficient and thermal conductivity, [see Bohn et al. (1995); Han et al. (2001)]. Some applications have been made with this method: Okita and Ymawaki (2002) made analysis for turbine rotor-stator system using commercial CFD code, film cooling applications were studied by Kusterer et al. (2006) using their in-house codes, and a transient study case can be found in Okita (2006) and He and Oldfield (2011).

As mentioned above, a fully conjugate code is a particularization of a CFD code, thus its efficiency as a heat transfer solver for the solid relies on the algorithms of the original CFD code, which were not actually designed to cope with this very specific problem. Another approach is to decouple the fluid and solid computing, using a specialized solid code to have better performance in the solid part. The loosely coupled method employs two separate codes to solve fluid and solid problems independently. In each coupling iteration, boundary information is exchanged between the two solvers. Upon convergence, the continuity of temperature and heat flux at the interface is also ensured. There are several approaches, depending on how the boundary information is changed, Dirichlet condition (wall temperature), Neumann boundary conditions (heat flux), or convective heat transfer condition to thermal code (via htc) can be used. Different methodology details can be found in papers Montenay and Duboue (2000); Verdicchio and Chew (2001); Divo et al. (2002); Verstraete et al. (2007); Verstraete and Van den Braembussche (2009). The loosely coupled method takes advantages that existing fully validated fluid and thermal codes can be directly used without modification. The designer could inherit the corresponding experiences and knowledge of the codes, which is important for industrial applications. In addition, it is flexible to couple different of fluid and solid codes. Vast number of applications of this method in turbomachinery can be found , use FEM [e.g. Illingworth and Hills (2005)], BEM [e.g. Heidmann et al. (2003)] or FVM [e.g. Corral et al. (2011a)] as the solid solver code. Extension to unsteady transient analysis have been made by Illingworth and Hills (2005) and Sun et al. (2010), where a steady state fluid solution is used to couple with unsteady solid FEM analysis for simulating the transient behavior in the solid. The main disadvantage of loosely coupled methods is that the CFD solver must be invoked many times in an iterative manner leading to relatively large computing times. This paper first performs an analysis of heat transfer coefficient Forward Temperature Backward (hFTB) loosely coupled method to study the convergence property. Then a new highly efficient and robust coupling method is proposed. Finally, an impingement cooling passage model and a stator well cavity are tested to compare the new method and conventional one .

### BASELINE SOLVER:

The present work is based on an in-house coupled fluid/solid code *FAUST*. It uses the most popular hFTB approach [e.g. Montenay and Duboue (2000); Verdicchio and Chew (2001); Verstraete et al. (2007)], which refers as heat transfer coefficient Forward Temperature Backward. This method applies the convective heat transfer boundary condition at solid domain and return wall temperature to fluid domain.

At the  $n^{th}$  iteration, the convective boundary condition at the solid domain:

$$q_{solid}^n = h(T_{w-solid}^n - T_{ref}^n) \quad (1)$$

Where the bulk temperature  $T_{ref}$  is calculated from fluid solution:

$$T_{ref}^n = T_{w-fluid}^n - \frac{q_{fluid}^n}{h} \quad (2)$$

The final expression:

$$q_{solid}^n - q_{fluid}^n = h(T_{w-solid}^n - T_{w-fluid}^n) \quad (3)$$

Eq. (3) shows that when the convergence state is achieved by having the same wall temperatures at the interface of both part, the flux continuity condition will be ensured as well. The value of heat transfer coefficient does not influence the final result. However, a positive heat transfer coefficient has to be ensured to avoid the physical meaningless and ill-posed problems in the heat conduction, Montenay and Duboue (2000). The current experiences of hFTB method recommend to use a larger constant positive htc value for all the nodes to avoid stability problem, see Verstraete et al. (2007).

*FAUST* code couples the in-house CFD code  $Mu^2s^2T$  and thermal code *Mephisto* as fluid and solid solver. Validation case can be found in paper of Corral et al. (2011a).

The CFD code  $Mu^2s^2T$ , see Burgos et al. (2011), developed mainly for turbomachinery applications, solves the compressible Navier-Stokes equation in conservative form for an arbitrary control volume, which may be written in compact form as:

$$\frac{d}{dt} \int_{\Omega} \mathbf{U} d\Omega + \int_{\Sigma} \mathbf{F}(\mathbf{U}) \cdot d\mathbf{A} = 0 \quad (4)$$

where  $\mathbf{U}$  is the vector of conservative variables,  $\mathbf{F}$  the sum of the flux,  $\Omega$  the flow domain,  $\Sigma$  its boundary and  $d\mathbf{A}$  the differential area pointing outward to the boundary. The solver uses hybrid unstructured grids to discretise the spatial domain and may contain cells with an arbitrary number of faces. The solution vector is stored at the vertexes of the cells. [Addressing Rev3-B2](#): Turbulence effects are modeled using the  $k-\omega$  turbulence model, Wilcox (1998). The basic time-stepping scheme is an explicit five stage Runge-Kutta scheme, where the artificial viscosity and the viscous terms are evaluated only in three stages. Local time stepping is used to enhance the convergence acceleration. The residuals are smoothed implicitly by a Jacobi iteration scheme in order to increase the support of the space discretisation as well. Low Mach number preconditioning is also used to accelerate convergence to steady state. Multigrid and parallel techniques are used to reduce the turn around time.

The thermal solver *Mephisto*, see Corral et al. (2011b), solves heat conduction equation for the solids.

$$\int \rho c \frac{dT}{dt} = \int_{\Sigma} \mathbf{q} \cdot d\mathbf{A} + \int_{\Omega} Q d\Omega \quad (5)$$

where  $q$  is the heat flux and  $Q$  is the volumetric heat sources. The spatial discretization is the same as the CFD solver. The set of equations are solved using a SOR method. Transients are marched in time by a Crank-Nicholson scheme.

## ANALYSIS USING 1D MODEL

There is nearly no paper can be found to discuss the computational time cost of loosely coupled heat transfer method. Depending on cases or number of CFD iterations for each boundary information exchange, time cost can be quite different. Besides, stability problems may appear as well, if the CFD does not converge properly in practical applications. Here we consider a 1D coupled heat transfer mode to study only the procedure of boundary information exchange. The sketch of the model is shown in Fig. 1. Assume the heat transfer only conducts along  $x$  direction. Wall temperature  $T_0$  is specified at the non-coupled side of the solid part,  $k$  is the thermal conductivity of solid material, and  $l$  represents the characteristic length of the solid model. In the fluid part,  $T_{ref}$  is the local bulk temperature,  $T_{wall}$  and  $q$  are the wall temperature and heat flux through the wall.

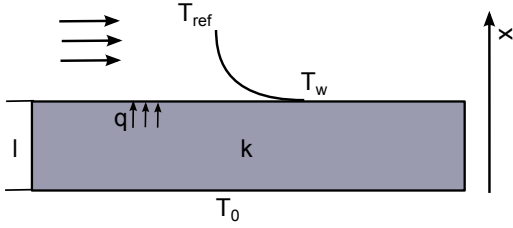


Figure 1: 1D coupled fluid/solid heat transfer model

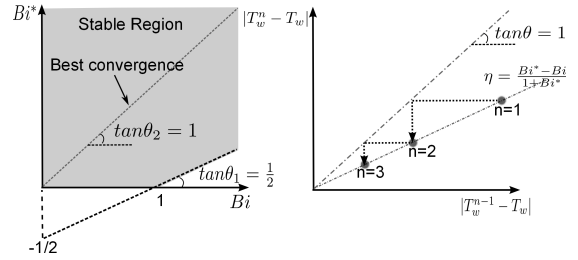


Figure 2: 1D mode stability region and convergence scheme of hFTB method

Consider the hFTB scheme, it allows to use arbitrary positive number of heat transfer coefficient. For the sake of clarity, assume  $h$  represents the physical real heat transfer coefficient in the coupling problem. And use  $h^*$  as the artificial value for computing. Then for hFTB method in 1D problem, the solution of the fluid part can be written as Eq. (6), and the solid 1D heat conduction can be expressed as Eq. (7)

$$q_{w-fluid} = h(T_w - T_{ref}) \quad (6)$$

$$q_{w-solid} = -\frac{k}{l}(T_w - T_0) \quad (7)$$

Suppose the initial wall temperature applied to fluid solver has  $\Delta T$  difference from the real wall temperature,

$$T_w^{initial} = T_w + \Delta T \quad (8)$$

Substitute Eq. (8) this to Eq. (6) to calculate  $T_{ref}$

$$T_{ref}^1 = T_w + \Delta T - \frac{q_{w-fluid}}{h^*} \quad (9)$$

The convective boundary condition to solid is introduced by using artificial htc  $h^*$ , since the real one is unknown

$$q_{w-solid}^1 = h^*(T_w^1 - T_{ref}^1) \quad (10)$$

using Eq. (7) and Eq. (10) to solve and get  $T_w^1$  and repeating the process, we get at the  $n^{th}$  iteration

$$T_w^n = T_w + \left(\frac{Bi^* - Bi}{1 + Bi^*}\right)^n \Delta T \quad (11)$$

and

$$T_w^n - T_w = \eta(T_w^{n-1} - T_w) \quad (12)$$

where  $Bi = hl/k$  is the Biot number,  $Bi^* = h^*l/k$  is the corresponding virtual Biot number and defining  $\eta = \left(\frac{Bi^* - Bi}{1 + Bi^*}\right)$  is the convergence efficiency. According to Eq. (11), hFTB method is unconditionally stable when  $Bi \leq 1$ , and stable if  $Bi^* > \frac{Bi-1}{2}$ , when  $Bi > 1$ . The stable region and convergence scheme is plotted in Fig. 2. As shown in the figure, when  $Bi^*$  moves closer to  $Bi$ ,  $\eta$  reduces, the required convergence iteration number will decrease without stability problem. If the  $Bi^*$  is the same as  $Bi$ , convergence achieves in next iteration. Since the stable condition in term of Biot number is equivalent as [Addressing Rev1-A2](#):  $h^* > \frac{h}{2}$ , the scheme can be controlled via  $h^*$ . When the  $h^*$  value is moving closer to the  $h$ , faster convergence rate is obtained. In addition, if the estimation of  $h^*$  is close to the real  $h$ , no stability problem will be encountered. This explains why hFTB method is more stable than others since a large  $h^*$  is taken in current experiences. Similar analysis and results of other kinds of loosely coupled method can also be found in paper of Verstraete and Van den Braembussche (2009).

## PROPOSED METHOD

The conventional approach of hFTB method uses a large constant value  $h^*$  everywhere to ensure stability, (Montenay and Duboue (2000); Verstraete et al. (2007); Verstraete and Van den Braembussche (2009); Corral et al. (2011a)). However, in 3D turbomachinery applications, htc are not uniform and can show large spatial non uniformities. According to Eq. (11), the convergence rate will be very slow in the conventional method. Alternatively if  $h^*$  is adjusted locally, both in time and space, the convergence process will be faster and stability problems can be avoided. However, it is not easy to find a reasonable  $h^*$  distribution before the computation, hereby we propose a dynamic updating of the virtual htc which is calculated automatically during the coupling process. The implementation dynamic virtual htc is described as follows:

Eq. (11) assumes that both the fluid and the solid solvers provide the correct response to the applied boundary condition and therefore is only valid when the solvers are run until convergence. The flow chart of the dynamic htc approach implemented in *FAUST* is shown in Fig. 3. It starts from a solution of the solid solver with adiabatic or other conditions to obtain a wall temperature distribution for CFD. Since the virtual htc distribution is unknown, during the first and second iterations,  $h^*$  still uses a constant value as described in the baseline method. From the end of the second iteration, the  $h^*$  is dynamically re-calculated using the current and pre-stored CFD result to obtain a more realistic value for next iteration, as shown in Eq. (13).

$$h_{n+1}^* = \frac{dq}{dT_w} = \left| \frac{q^{n-1} - q^n}{T_w^n - T_w^{n-1}} \right| \quad (13)$$

The updating of the virtual htc stops when the wall temperature variations are smaller than a specified threshold  $\beta$ , normally is 3K, between two iterations. At this point, consider that  $h^*$  is close enough to  $h$ . Local limitations of maximum and minimum  $h^*$  are set to ensure not obtaining meaningless values for  $h^*$ , [Addressing Rev2-A1](#) where  $h_{max}^* = 6 \text{ mW/mm}^2\text{K}$ ,  $h_{min}^* = 0.01 \text{ mW/mm}^2\text{K}$ .

## CASE STUDY

Two representative of turbomachinery applications have been carried out in order to test the efficiency and robustness of the proposed method in realistic 3D cases.

**Impingement model** A simple internal impingement cooling model is showing in Fig. 4. The model consists of two flow channels, connected through ten staggered arranged impingement cooling

holes. The coolant flow enters from the root of the mid-chord passage and then pass through the impingement hole to cool the leading wall of the front passage channel. The flow leaves from the tip of the front passage. The solid model is located at the leading edge and coupled with the fluid domain through the three surfaces of the front channel to investigate the coupled heat transfer effects. The rest of the surfaces which are uncoupled with the fluid are assumed to be adiabatic.

Both the fluid and solid meshes have been created using the same in-house grid generator using tetrahedral elements. Prismatic layers are generated first before the creation of the volumetric grid in the fluid domain. The computational model has around 0.25 million nodes in the fluid domain and 8,000 nodes in the solid domain. The inlet total pressure is 130kPa, total temperature is 600K and the inlet turbulent kinetic energy is 3%. The leading surface of the solid model is set to a constant temperature of 1150K. Wilcox's  $k - \omega$  turbulence model (Wilcox, 1998) is used to account for turbulent effects.

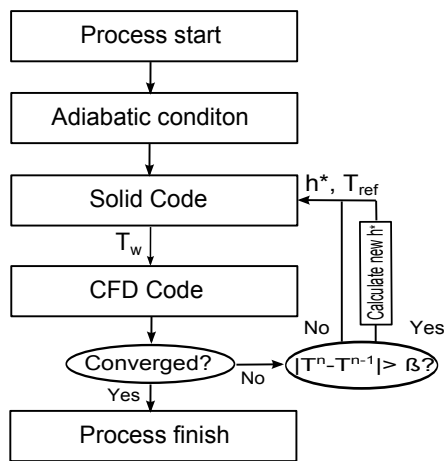


Figure 3: Scheme of dynamic htc approach of hFTB method

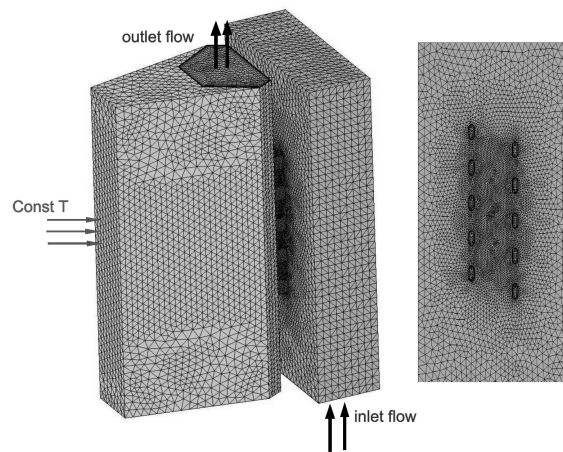


Figure 4: Addressing Rev1-A5 A6 3D impingement model

**Turbine stator well model** This turbine stator well model was taken from EU FP6 project MAGPI. This case has been previously studied to validate the coupled heat transfer code. It was shown (see Corral et al. (2011a)) that the accuracy of the coupled simulation was better than that of the uncoupled approach against existing experimental data. Fig. 5 displays the geometry of the stator and the associated front and rear cavities. The 3D coupled heat transfer simulation uses a single pitch of the stator array, and the disk holes have been substituted by a slot of equivalent area. The stator is coupled with the fluid domain, while the temperature distribution along the rotating parts is taken from experimental data.

Model	Test 1: constant $h^*$	Test 2: constant $h^*$	Test 3: new dynamic $h^*$
Impingement model	$h^* = 1mW/mm^2K$	$h^* = 3mW/mm^2K$	dynamic, using $h^* = 1mW/mm^2K$ for starting
MAGPI case model	$h^* = 1mW/mm^2K$	$h^* = 3mW/mm^2K$	dynamic, using $h^* = 1mW/mm^2K$ for starting

Table 1: Artificial htc value used for coupling analysis

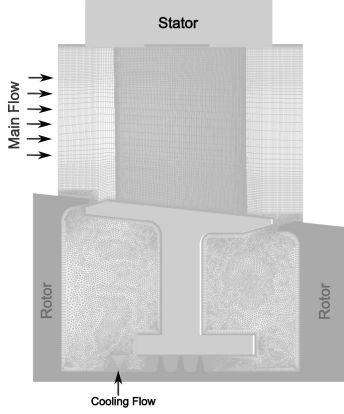


Figure 5: MAGPI turbine stator well model

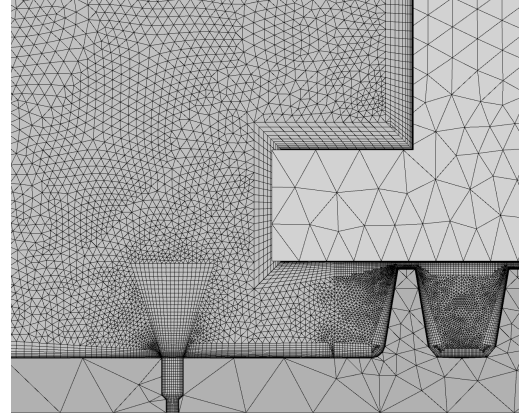


Figure 6: Mesh detail for CFD and solid domains at the labyrinth seal and inlet cooling flow.

Main and the cooling flow inlet conditions are taken from the experimental data (main an cooling flow inlet total temperature are about 385K and 350K respectively, rotor rotating speed is 10630 rpm, stator inlet mass flow is 4.8 kg/s, and the inlet total pressure around 3 bar). The static pressure of the main flow exit and the total pressure of the cooling flow inlet are adjusted to match the measured mass flows. Wilcox's  $k - \omega$  turbulence model (Wilcox, 1998) is used as well in this simulation. The grid size of the CFD model is about 3.15 million nodes while the solid model of the stator contains just 13,000 nodes. The surface mesh of the two models are not consistent, so that an linear interpolation will be used to transmit the boundary data between two codes. Fig. 6 shows a closeup of the numerical model at the labyrinth seal area.

Both cases are tested in three test conditions. As shown in Tab. 1 First two tests use the conventional method, with two constant  $h^*$ , where the value in Test 2 is the default setting hFTB method. Test 3 uses the new dynamic  $h^*$  approach. The impingement model was run in a single processor, while the MAGPI model was run in a cluster using ten partitions.

## RESULT AND DISCUSSION

Fig. 7 and Fig. 8 plot the results of the coupled wall temperature and heat transfer coefficient filed of two models. All the three tests are providing exactly the same results for the temperature field. As the hFTB method described, the value of artificial htc does not influence the final result. The results for the stator well cavity are the same as previously reported (Corral et al., 2011a). For the leading edge impingement cooling model the signature of the impinging jets is clearly seen in the htc contour plots (Fig. 7). However the discussion of the results is not the main purpose of this work but the computational efficiency of the proposed method.

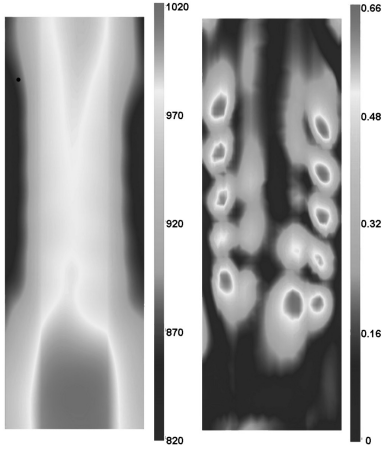


Figure 7: Impingement model coupling surface temperature distribution ( $K$ ) and heat transfer coefficient distribution ( $mW/mm^2K$ )

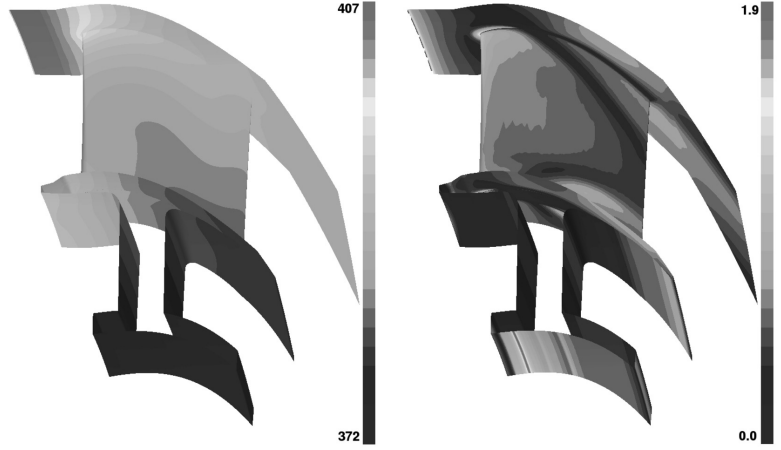


Figure 8: MAGPI stator well model coupling surface temperature distribution ( $K$ ) and heat transfer coefficient distribution ( $mW/mm^2K$ )

**Convergence behavior:** The convergence histories of the two models as a function of the number of coupling iterations are presented in Fig. 9, and Fig. 10. The vertical axis is represented in logarithmic scale. The error factor  $\varepsilon$  is defined as:

$$\varepsilon = \frac{1}{(T_{max} - T_{min})} \sqrt{\frac{1}{N} \sum_{i=1}^N (T_{w,i}^n - T_{w,i}^{n-1})^2} \quad (14)$$

with  $N$  the number of coupling boundary nodes, and  $T_{max}$  and  $T_{min}$  are the maximum and minimum wall temperatures. All the errors are set to zero at first iteration for clarity. According to Eq. 12, the slope of the convergence history in Test 1 and 2 shall be constant in logarithmic scale. This is because  $\eta$  is fairly constant if the real htc distribution does not change much during computing. The two models both exhibit a similar convergence history as the 1D analysis predicted that Test 1 needs fewer iterations than Test 2 because its  $h^*$  is closer to the actual physical mean htc.

Test 3 gives the smallest number of convergence iterations. As the htc distribution is unknown at the first two iterations, the same constant  $h^*$  as in Test 1 is used. Hence, the result are the same in Test 1 and Test 3 at the first two iterations. From the third iteration where dynamic htc is applied, the slope varies significantly and goes down as the number of iteration increase. Then it becomes nearly constant again and with much larger slope than the test 1, from where consider that the htc variation becomes small.

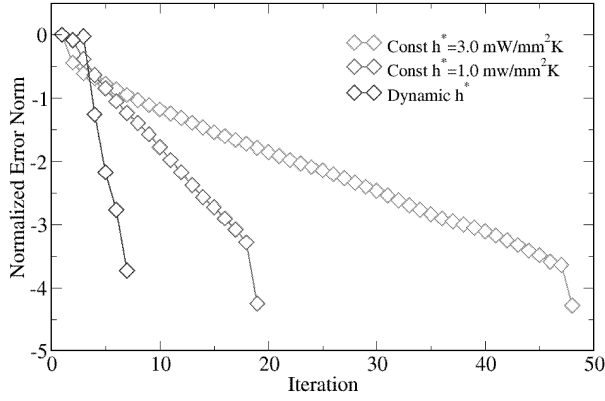


Figure 9: Impingement model convergence history plot

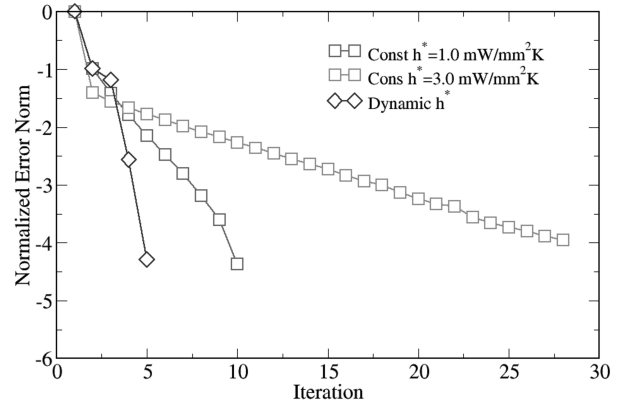


Figure 10: MAGPI stator well model: convergence history plot

**Computational time:** The computational time cost for the impingement and stator well cavity models are shown in Fig. 11 and Fig. 12 respectively. For each model, the same computer resources and settings are used for all the three cases in order make the computational time being comparable. The computational cost is normalized with the cost of the initial stand-alone CFD simulation in the following way

$$t_{nor} = \frac{t_{coupling}}{t_{1st.cfd}} \quad (15)$$

Since the cost of the first CFD solution spends around the same amount of time as the equivalent uncoupled solution, the ratio represents as well the relative cost between a fully coupled and an uncoupled solutions.

Again for the cases with constant  $h^*$ , the one that is closer to the physical htc converges faster. The dynamic cases consumes less than 2.5 times the cost of a stand-alone CFD calculation but with the same accuracy as conventional method. In all the tests, most of the computing time are spent on the initial few iterations because the variation of temperature between iterations is relatively large and CFD needs more time to get converged. And the time spent to converge the CFD solutions at the latest stages of the convergence process are very small. This may be appreciated both in Figs. 11 and 12 where all the iterations are represented in the graph with a symbol and it may be observed that the latest iterations does not make an additional cost because are converged in a very small time.

In the conventional method, the determination of virtual htc distribution can be difficult to predict without a very good knowledge of the problem. The dynamic htc approach not only is much faster but more robust. Moreover it is easier to devised automatic methods without the input of the end-users. The dynamic method is faster than the conventional one for two reasons: First, the disparity of htc values along the wet surfaces may be automatically taken into account. This frees the method for an automatic selection of the virtual heat transfer solution taking into account the local characteristics of the different flow regions. Otherwise when there are large differences in the htc distribution the monolithic approach based on the existence of a single virtual htc induces necessarily a penalty in the method since it is impossible to find out the optimum solution. Second, even in the case that htc were constant, the method provides a mechanism to find out the optimum virtual htc. As a result, the dynamic method is about two to three times faster than the conventional method.

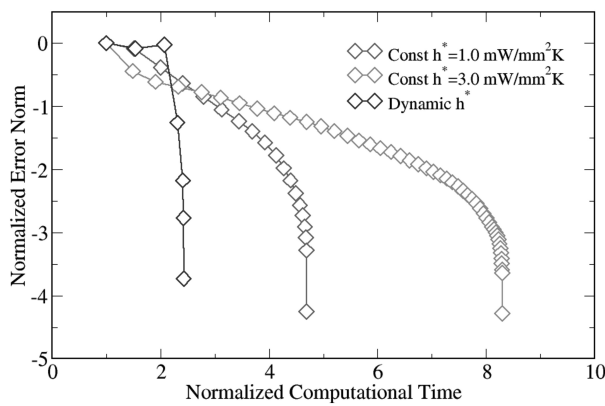


Figure 11: Impingement model: convergence time plot

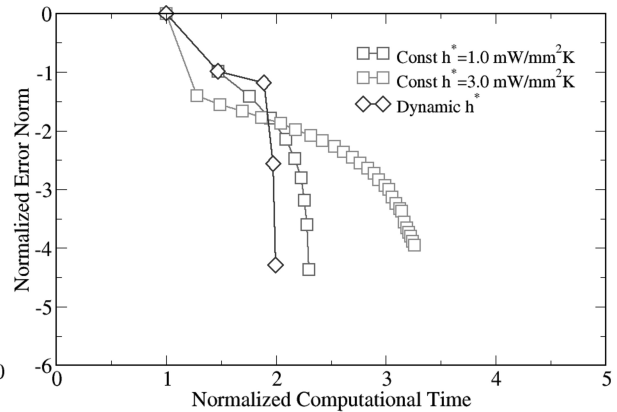


Figure 12: MAGPI stator well model: convergence time plot

## CONCLUSIONS

This paper proposes a new dynamic htc approach to reduce the computational time of loosely coupled fluid/solid heat transfer method that reduces the computing time by a factor of two to three. Convergence analysis based in a simple one-dimensional model shows that, in heat transfer coefficient Forward Temperature Backward (hFTB) method, the convergence behavior is influenced by the physical Biot number and can be controlled by a user specified virtual htc. The closer the virtual htc distribution is to the physical one, the faster the convergence rate.

The new method provides a dynamic updating process for seeking the optimal virtual htc, which is the physical one. Further more, it frees the consideration of stability problems. The two 3D case studies show that the 1D stability criteria can be used for realistic 3D cases as well. The dynamic htc approach provides faster convergence than the conventional one.

The new method only spends less than 2.5 times computing time of a stand-alone CFD solution to obtained coupled heat transfer solutions, making the coupled method very attractive from an industrial point of view. This new method is beneficial as well to a coupled transient analysis, since the building of transient analysis is the static coupled heat transfer that takes place at every single time step of the transient.

## ACKNOWLEDGMENTS

The data of stator well cavity model was supported by the European Commission within the Framework 6 Program, Research Project Main Annulus Gas Path Interactions (MAGPI), AST5-CT-2006-030874. The authors wish to thank EU FP6 program for their support and permission to use the experimental data and publish the paper. The authors also want to thank “Industria de TurboPropulsores S.A.” for providing working resources and allowing publication of this paper.

## REFERENCES Addressing Rev2:A2

- Bohn, D., Schonenborn, H., Bonhoff, B. and Wilhelmi, H. (1995). Prediction of the Film-cooling Effectiveness in Gas Turbine Blades Using a Numerical Model for the Coupled Simulation of Fluid Flow and Diabatic Walls, *ISABE95 Paper, no. ISABE95-7105*.
- Burgos, M., Contreras, J. and R., C. (2011). Efficient edge-based rotor/stator interaction method, *AIAA journal* (49:19-31).

- Corral, R., Chaquet, J., Pastor, G., Pueblas, J. and Coren, D. (2011a). Validation of a Coupled Fluid/Solid Heat Transfer Method, *ASME Paper, no. GT2011-45951*.
- Corral, R., Pastor, G. and Contreras, J. (2011b). Turbomachinery thermal analysis using coupled two and three dimensional model and reduced order fluid models, *ASME Paper, no. GT2011-45998*.
- Divo, E., Steinthorsson, E., Kassab, J. and Bialecki, R. (2002). An Iterative BEM/FVM Protocol for Steady State Multi-Dimensional Conjugate Heat Transfer In Compressible Flows, *Eng. Anal. Bound. Elem.* pp. 447–454.
- Han, Z., Dennis, B. and Dulikravich, G. (2001). Simultaneous Prediction Of External Flow-Field And Temperature In Internally Cooled 3-D Turbine Blade Material, *Int J. Turbo Jet-Engines* **133**: 47–58.
- He, L. and Oldfield, M. (2011). Unsteady Conjugate Heat Transfer Modeling, *ASME J. of Turbomach.* **133**: 031022–1–12.
- Heidmann, J., Kassab, A., Divo, E., Rodriguez, F. and Steinthorsson, E. (2003). Conjugate Heat Transfer Effects on a Realistic Film-Cooled Turbine Vane, *ASME Paper, no. GT2003-38553*.
- Illingworth, J. B. and Hills, N. J. (2005). 3D Fluid-Solid Heat Transfer Coupling of an Aero Engine Pre-Swirl System, *ASME Paper, no. GT2005-68939*.
- Kusterer, K., Hagedorn, T., Bohn, D., Sugimoto, T. and Tanaka, R. (2006). Improvement of a Film-Cooled Blade by Application of The Conjugate Calculation Technique, *ASME J. of Turbomach.* **128**(3): 572–578.
- Montenay, A. and Duboue, J. (2000). Conjugate Heat Transfer Analysis of an Engine Internal Cavity, *ASME Paper, no. 2000-GT-282*.
- Okita, Y. (2006). Transient Thermal and Flow Field in a Turbine Disk Rotor-Stator System, *ASME Paper, no. GT2006-90033*.
- Okita, Y. and Ymawaki, S. (2002). Conjugate Heat Transfer Analysis of Turbine Rotor-Stator System, *ASME Paper, no. GT-2002-30615*.
- Rigby, D. and Lepicovsky, J. (2001). Conjugate Heat Transfer Analysis of Internally Cooled Configurations, *ASME Paper, no. 2001-GT-0405*.
- Sun, Z., Chew, J.W. and Hills, N., Volkov, K. and Barnes, C. (2010). Efficient Finite Element Analysis / Computational Fluid Dynamics Thermal Coupling for Engineering Applications, *ASME J. of Turbomach.* **132**(3): 031016–1–9.
- Verdicchio, J. and Chew, J.W. and Hills, N. (2001). Coupled Fluid/Solid Heat Transfer Computation for Turbine Discs, *ASME Paper, no. 2001-GT-0205*.
- Verstraete, T., Alsalihi, Z. and Van den Braembussche, R. (2007). Numerical Study of the Heat Transfer in Micro Gasturbines, *ASME J. of Turbomach.* **129**(4): 835–841.
- Verstraete, T. and Van den Braembussche, R. (2009). A Novel Method For The Computation of Conjugate Heat Transfer With Coupled Solvers, *Ichmt. Digital Library Online* .
- Wilcox, D. C. (1998). Turbulence Modeling for CFD, *DCW Industries, Inc, California*.